






Category: STEM (Science, Technology, Engineering and Mathematics)

ORIGINAL

Enhance the properties of the stainless steel Solar basin by using new ceramic coatings

Mejorar las propiedades del lavabo Solar de acero inoxidable utilizando nuevos revestimientos cerámicos

Elham A. Majeed¹ , Hayder K. Rashid¹ , Saja F. Abdul Hadi² 

¹Doctor at Babylon University, College of Materials Engineering. Iraq.

²Master's student at Babylon University, College of Materials Engineering. Iraq.

Cite as: Majeed EA, Rashid HK. Enhance the properties of the stainless steel Solar basin by using new ceramic coatings. Salud, Ciencia y Tecnología - Serie de Conferencias. 2024; 3:838. <https://doi.org/10.56294/sctconf2024838>

Submitted: 25-01-2024

Revised: 05-04-2024

Accepted: 02-06-2024

Published: 03-06-2024

Editor: Dr. William Castillo-González 

Note: paper presented at the 3rd Annual International Conference on Information & Sciences (AICIS'23).

ABSTRACT

Solar energy is increasingly being used as a renewable energy source in water analysis, energy devices, treatment systems, data logging, and analytical instruments, providing sustainable and cost-effective solutions. A 316 stainless steel sink was utilized with the aim of enhancing its thermal insulation properties. Ceramic materials such as mullite ($3\text{Al}_2\text{O}_3 \cdot 2\text{SiO}_2$), titanium dioxide (TiO_2), and magnesium oxide (MgO) are identified as effective insulating agents for improving the insulation processes of a stainless steel 316 basin. Mullite powder is added in weight ratios of 0,7 %, 2,21 %, 3,79 %, and 3,78 %. Titanium dioxide is also added in weight ratios of 0,3 %, 0,79 %, 1,39 %, and 0,7 %. To enhance the insulation ratio, add 0,6 % magnesium oxide to S5. The coating process involves air-brush painting on the stainless steel sheet to ensure a uniform and durable application. Various tests, including X-ray diffraction (XRD), scanning electron microscopy (SEM), atomic force microscope (AFM), thermal conductivity measurement, adhesion strength testing, density measurement, coating thickness analysis, evaluation of UV radiation resistance, and porosity determination, are conducted to evaluate the performance and characteristics of the coatings. Thermal insulation was achieved for sample S4, resulting in a thermal conductivity value of $0,231411 \text{ W/m} \cdot ^\circ\text{C}$, along with an associated increase in pore percentage of 0,88 %. Additionally, sample S4 exhibited a lower density value of $1,22 \text{ kg/m}^3$, attributed to the incorporation of oxide. In comparison, sample S5, composed of magnesium, exhibited the highest thickness among the remaining samples, measuring ($540\mu\text{m}$). The project's objective is to create a sustainable and enhanced method for water desalination by leveraging renewable energy sources and advanced insulation techniques incorporating ceramic coatings. This innovative approach aims to decrease energy consumption and minimize environmental repercussions, thereby facilitating the provision of safe drinking water, particularly in regions grappling with water scarcity. Additionally, the project seeks to enhance the properties of a stainless steel 316 basin by reducing thermal conductivity, ultimately increasing the insulation percentage. This endeavor involves harnessing solar energy as a means of achieving these goals.

Keywords: Thermal Insulation; Stainless Steel 316; Desalination Basin; Mullite ($3\text{Al}_2\text{O}_3 \cdot 2\text{SiO}_2$); Titanium Oxide (TiO_2); Magnesium Oxide (MgO); Spray Airbrush.

RESUMEN

La energía solar se utiliza cada vez más como fuente de energía renovable en análisis de aguas, dispositivos energéticos, sistemas de tratamiento, registro de datos e instrumentos analíticos, proporcionando soluciones

sostenibles y rentables. Se utilizó un fregadero de acero inoxidable 316 con el objetivo de mejorar sus propiedades de aislamiento térmico. Materiales cerámicos como la mullita ($3\text{Al}_2\text{O}_3 \cdot 2\text{SiO}_2$), el dióxido de titanio (TiO_2), y el óxido de magnesio (MgO) se identifican como agentes aislantes eficaces para mejorar los procesos de aislamiento de un lavabo de acero inoxidable 316. Se añade polvo de mullita en proporciones de peso de 0,7 %, 2,21 %, 3,79 %, y 3,78 %. También se añade dióxido de titanio en proporciones de 0,3 %, 0,79 %, 1,39 % y 0,7 %. Para mejorar la proporción de aislamiento, se añade óxido de magnesio al S5 en un 0,6 %. El proceso de revestimiento consiste en pintar con aerógrafo la chapa de acero inoxidable para garantizar una aplicación uniforme y duradera. Para evaluar el rendimiento y las características de los revestimientos, se realizan varias pruebas, como difracción de rayos X (DRX), microscopía electrónica de barrido (SEM), microscopio de fuerza atómica (AFM), medición de la conductividad térmica, pruebas de resistencia a la adherencia, medición de la densidad, análisis del espesor del revestimiento, evaluación de la resistencia a la radiación UV y determinación de la porosidad. Se consiguió el aislamiento térmico de la muestra S4, lo que dio lugar a un valor de conductividad térmica de $0,231411 \text{ W/m} \cdot ^\circ\text{C}$, junto con un aumento asociado del porcentaje de poros del 0,88 %. Además, la muestra S4 presentaba un valor de densidad inferior de $1,22 \text{ kg/m}^3$, atribuido a la incorporación de óxido. En comparación, la muestra S5, compuesta de magnesio, exhibió el mayor espesor entre las muestras restantes, midiendo ($540 \mu\text{m}$). El objetivo del proyecto es crear un método sostenible y mejorado para la desalinización del agua aprovechando las fuentes de energía renovables y las técnicas avanzadas de aislamiento que incorporan revestimientos cerámicos. Este enfoque innovador pretende reducir el consumo de energía y minimizar las repercusiones medioambientales, facilitando así el suministro de agua potable segura, sobre todo en regiones que luchan contra la escasez de agua. Además, el proyecto pretende mejorar las propiedades de una pila de acero inoxidable 316 reduciendo la conductividad térmica y, en última instancia, aumentando el porcentaje de aislamiento. Para alcanzar estos objetivos se aprovechará la energía solar.

Palabras clave: Aislamiento Térmico; Acero Inoxidable 316; Balsa de Desalinización; Mullita ($3\text{Al}_2\text{O}_3 \cdot 2\text{SiO}_2$); Óxido de Titanio (TiO_2); Óxido de Magnesio (MgO); Aerografía de Pulverización.

INTRODUCTION

Water scarcity is a significant global issue, despite the abundant presence of water on Earth. Desalination technologies have emerged as potential solutions to address the shortage of safe drinking water.⁽¹⁾ The desalination process involves removing excess salts from seawater or brackish water to make it suitable for use and drinking, and it can be achieved through thermal or membrane processes.⁽²⁾ Renewable energy sources (RES) offer sustainable and environmentally friendly alternatives to fossil fuels. They contribute to reducing greenhouse gas emissions and promoting local socio-economic development.⁽³⁾ However, the development of renewable energy projects requires careful consideration of environmental trade-offs and public acceptance.⁽⁴⁾ Solar power and wind power are currently the primary renewable energy sources being considered.⁽⁵⁾ Mullite has a thermal conductivity of $3,3 \text{ W/m} \cdot \text{K}$ and a coefficient of thermal expansion of $5,3 \times 10^{-6} \text{ K}^{-1}$.^(6,7) Titanium oxide (TiO_2) has a thermal conductivity of $3,3 \text{ W/m} \cdot \text{K}$ and a thermal expansion value of $9,4 \times 10^{-6} \text{ K}^{-1}$.⁽⁸⁾ Magnesium oxide (MgO) has a thermal conductivity ranging from approximately $3,0$ to $6,0 \text{ W/m} \cdot \text{K}$ and a coefficient of thermal expansion (CTE) typically ranging from 10 to $15 \times 10^{-6} / ^\circ\text{C}$.⁽⁹⁾ Composite materials, combining ceramic and polymer components, can be used for coating purposes.⁽¹⁰⁾

Stainless steel alloy 316, known for its corrosion resistance and high-temperature strength, it can be coated with an insulation film to enhance its heat resistance properties.⁽¹¹⁾ Mechanical treatments such as electrostatic discharge manufacturing (EDM), heat treatment, surface roughening, and plasma oxidation can improve the adhesion strength of stainless steel.^(12,13) A spray gun is commonly used to apply coatings, as it atomizes the coating material into small particles and propels them onto the surface.⁽¹⁴⁾ An air compressor is used to pressurize the air and create the force required to propel the coating material.⁽¹⁵⁾ Thermal insulation of stainless steel can be achieved by applying a ceramic coating. Methods such as casting, vacuuming, surface treatment, spray coating, baking, and high-temperature sintering can be employed for coating application.⁽¹⁶⁾ The ceramic layer acts as an insulation barrier, preventing direct contact between the stainless steel and the environment.⁽¹⁷⁾ Ceramic particles with low thermal conductivity are used in the coating to minimize heat or cold loss and reduce thermal radiation energy. The utilization of ceramic waste and solid particulates in the coating can improve thermal insulation and reduce costs. Coatings can be applied to stainless steel containers, building materials, and storage tanks to lower surface temperatures.⁽¹⁹⁾ Roughening the surface of stainless steel, achieved through various methods, can enhance adhesion and improve coating performance.⁽¹⁸⁾

Literature References

Kalamazoo et al.⁽¹⁹⁾, in this study, the properties of magnesium oxide as a pigment in paper coatings were

evaluated. The focus was on assessing its performance in terms of brightness, opacity, gloss, smoothness, and ink absorptivity. The results showed that coatings with magnesium oxide exhibited equal brightness at different levels of substitution. The opacity of the coatings was found to be consistent, with maximum opacity achieved at specific ratios of magnesium oxide to other components. Magnesium oxide coatings demonstrated higher Gardner gloss values compared to other coatings. Improved smoothness was observed with certain levels of magnesium oxide in the mixture. Additionally, the coatings with magnesium oxide showed increased ink absorptivity, likely due to a less dense coating structure containing more pores. Overall, the study concluded that magnesium oxide has potential as a pigment in paper coatings, provided that challenges related to dispersion and coater rheology are addressed

S. Kumar et al.⁽²⁰⁾, in this study, researchers aimed to develop and optimize a low-cost manufacturing method for environmental barrier coatings (EBCs) using the slurry spray technique (SST). The focus was on achieving coating quality comparable to expensive traditional methods. They specifically investigated the mullite-nickel based coating with MgO as a liquid phase sintering (LPS) additive. Taguchi's experimental design was employed to optimize the technique and analyze the effects of process parameters such as sintering temperature, sintering time, and percentage of additives. The coating's adhesion strength was measured as the response parameter. The test results demonstrated satisfactory adhesion strength, comparable to coatings produced by traditional techniques like flame spray. The study highlights the potential of the slurry spray technique for producing high-quality EBCs in a cost-effective manner.

Xitang Wang et al.⁽²¹⁾, a study focused on enhancing thermal protective materials using an anti-insulation integrated light phenolic resin composite with ceramic microspheres. The addition of ceramic microspheres reduced material density, improved thermal insulation properties, and overall material performance. Optimal ablation resistance was achieved at a 30 % volume fraction of microspheres. The resulting composite material met performance requirements, offering reduced density, enhanced heat insulation, and improved ablation resistance. Higher microsphere content improved performance, with 20 % and 30 % volume fractions demonstrating the best overall performance.

Bharat Kumar Yadav et al.⁽²²⁾, this study investigates the use of absorbing materials to enhance the productivity of single basin solar stills for water purification. Different materials, including black rubber mat, black ink, and black dye, were tested. Results indicate that incorporating these materials can increase daily water productivity by 38 %, 45 %, and 60 % respectively, with black dye being the most effective. Further improvements in solar still design and efficiency are necessary for wider commercial adoption. (The study explores absorbing materials to improve the productivity of single basin solar stills. Black dye proves to be the most effective, increasing water productivity by 60 %. Additional enhancements are needed to make solar stills more practical and commercially viable.)

Falah Ibrahim Mustafa et al.⁽²³⁾, this experimental investigation examined the integration of an evacuated tube solar collector with a single basin-single slope solar still. The study conducted in Baghdad demonstrated a significant increase in daily productivity (35,63 %) and efficiency (10,97 %) compared to a passive still. The results highlight the potential for improving solar still performance by utilizing evacuated tube collectors, particularly in areas with high solar radiation. Efforts should be focused on optimizing the design of the solar basin to minimize exergy loss. (Integration of an evacuated tube solar collector with a solar still led to substantial improvements in daily productivity and efficiency. The study emphasizes the importance of weather conditions and optimizing the solar basin design.)

Bahaa Eddin Moharram et al.⁽²⁴⁾, this work presents the integration of a latent heat storage system with a single basin solar still (SBSS), resulting in a 4,54 % improvement in daily fresh water productivity. The storage system, utilizing a paraffin-CuO nanocomposite, successfully overcame challenges associated with using paraffin wax as a storage material. The economic analysis estimated a cost of \$0,25 per liter of fresh water when utilizing the storage unit. Recommendations for future research include exploring multiple storage tanks, testing different phase change materials with nanomaterials, and investigating the use of solar reflectors in conjunction with the SBSS. (Integration of a latent heat storage system with an SBSS increased fresh water productivity, with a cost of \$0,25 per liter. Future research should focus on multiple storage tanks, alternative phase change materials, and solar reflectors.)

Experimental work

This study aimed to enhance the thermal efficiency of a stainless steel sink by using specific ceramic materials for insulation and a glass cover. Different forms of insulation were tested, and experiments evaluated energy efficiency, temperature retention, and heat loss. The results provide recommendations for improving pond designs and achieving energy conservation in various applications.

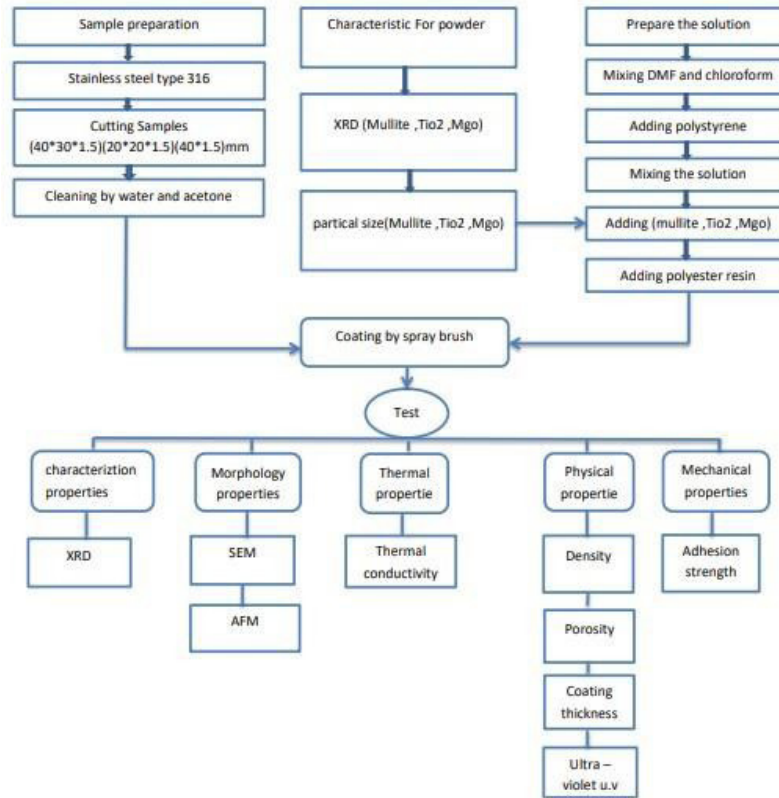


Figure 1. Showcases the experimental program utilized in the current research

Preparing the samples

Several steps are followed to prepare stainless steel type 316 plates for surface treatment and coating adhesion. Firstly, the stainless steel plate is cut into different shapes (rectangular: 40*30*1,5, square: 20*20*1,5, circular: diameter 40, thickness 1,5). The samples undergo cleaning using aston, a cleaning agent, to remove contaminants, oils, or residues. Distilled water is used to wash the samples after aston cleaning to eliminate any remaining cleaning agent traces. The surface is roughened using abrasive roughing paper to enhance mechanical bonding, increase surface area, and improve coating adhesion. Acetone and distilled water are used for subsequent cleaning, ensuring removal of any solvents or cleaning agents. Consistency in roughening is crucial. Following these steps, the stainless steel samples are properly prepared for coating

Used Materials

Ceramic materials (mullite, TiO_2 , MgO) were used to create a protective and insulating coating on a stainless steel sink. Mullite ($3\text{Al}_2\text{O}_3 \cdot 2\text{SiO}_2$) was chosen for its thermal stability and low thermal conductivity. Titanium dioxide (TiO_2) was included for its solar radiation reflectivity, reducing heat absorption. Magnesium oxide (MgO) contributed to insulation properties due to its low thermal conductivity. The ceramic coating was created by mixing the fine powders of mullite, TiO_2 , and MgO with binders (polyester resins), solvents (DMF, chloroform), and additives (polystyrene granules) to enhance adhesion and facilitate the coating application process. This research aims to optimize energy conservation by utilizing these ceramic materials in the coating applied to the stainless steel sink.

Preparing the coating mixture

Mullite, TiO_2 , and MgO powders are obtained. Additionally, polystyrene granules, solvents such as chloroform, dimethylformamide (DMF), and polyester resin (A,B) are utilized to enhance adhesion. XRD testing is conducted to verify the chemical composition and purity of the powders, as shown in the accompanying XRD graph. The solvents are combined and mixed together, and then polystyrene granules are added to the mixture. A magnetic stirring bar is used to stir the mixture for a duration of four hours until the polystyrene granules completely dissolve, resulting in a homogeneous gel. Polyester resin is subsequently added to the mixture by substituting a portion of it. To introduce different proportions of mullite into the mixture, the mullite is replaced in different quantities while the mixture is constantly stirred. In the first three samples, mullite is replaced by 25 % TiO_2 . As for the fourth sample, the mullite is replaced with both 12,5 % titanium oxide and 12,5 % magnesium oxide.

Samples	DMF	Chloroform	Polystyrene	Polyester Resin	Mullite	TiO ₂	MgO
S0	-	-	-	-	-	-	-
S1	39 %	39 %	14 %	7 %	-	-	-
S2	39 %	39 %	14 %	7 %	1 %	25 % from mullite	-
S3	38 %	38 %	14 %	7 %	3 %	25 % from mullite	-
S4	38 %	38 %	14 %	7 %	5 %	25 % from mullite	-
S5	38 %	38 %	14 %	7 %	5 %	12,5 % from mullite	12,5 % from mullite

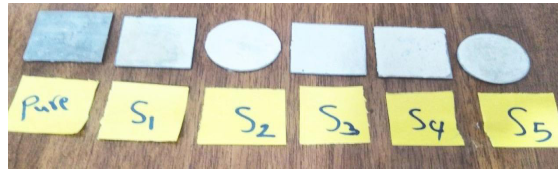


Figure 2. shows samples with insulator coating applied

Spray Coating (Airbrush Gun)

Spray coating, specifically using an airbrush gun, is a technique employed to apply a thin and controlled layer of coating material onto a surface. The airbrush gun operates by using compressed air to atomize the coating material into fine droplets, which are then evenly sprayed onto the target surface. The process starts by loading the coating material, such as paint or a liquid mixture, into the airbrush gun's reservoir. The gun is typically connected to an air compressor or a canister of compressed air. When the trigger is pressed, the compressed air is released, creating a vacuum that draws the coating material into a nozzle. As the coating material passes through the nozzle, it is atomized into a spray of tiny droplets. The distance between the airbrush gun nozzle and the surface being coated, as well as the spray speed, are critical factors in achieving an even and controlled application. The distance between the nozzle and sample surface is about 15 cm. The nozzle pinhole is about 1,5 mm. Proper adjustments ensure that the coating is distributed uniformly without excessive build-up or overspray. Spray coating with an airbrush gun offers several advantages. It allows for precise control over the thickness and coverage of the coating, making it suitable for applications that require fine details or intricate patterns. However, it is important to note that spray coating with an airbrush gun may have limitations depending on the viscosity and properties of the coating material. It is crucial to select the appropriate:

- Airbrush gun.
- Nozzle size.
- Air pressure settings to achieve the desired results.



Figure 3. (a) air compressor for spraying with an airbrush, (b) the system of the spray airbrush gun

Overall, spray coating using an airbrush gun is a versatile and efficient method for applying coatings, offering control, precision, and versatility in a wide range of applications.

RESULTS AND DISCUSSION

Characterization Properties before coating

X-ray diffraction (XRD) test: XRD analysis was performed on mullite powder, titanium dioxide and magnesium oxide samples to study their crystal structure and composition using the X-ray diffraction pattern. which are $(3Al_2O_3 \cdot 2SiO_2)$, the reference card (00-048-0075), Titanium dioxide material is observed according to the reference card (96-153-9683) in a chemical formula (TiO_2) and the diffraction pattern should exhibit peaks corresponding to the cubic crystal lattice structure of magnesium oxide. the reference card (01-089-4248) as shown in figure 4.

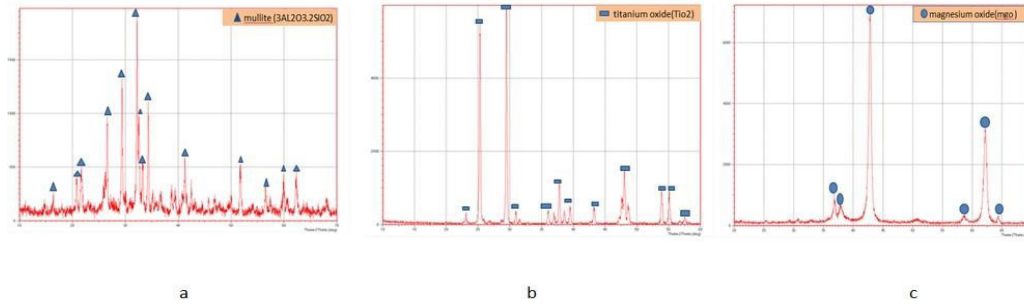


Figure 4. The (XRD) test analysis for powder. (a) Mullite (b) TiO_2 (c) MgO

Particle Size Analysis Test: particle size analysis tests were performed on mullite, titanium dioxide, and magnesium oxide powders to determine the particle size distribution.

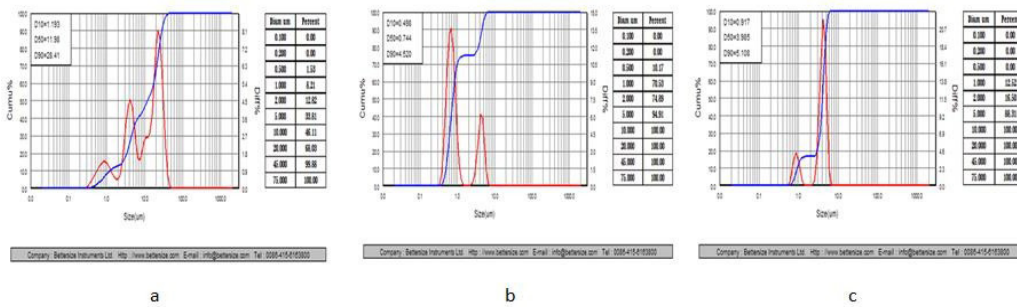


Figure 5. Show particle size analysis of powder materials. (a) Mullite. (b) TiO_2 . (c) MgO

Characterization Properties after coating

X-ray diffraction (XRD) test: the XRD analysis provided valuable information about the composition and structural properties of the samples. By examining the diffraction patterns, specific crystalline phases and their relative abundances could be identified. Sample S4, consisting of Mullite $(3Al_2O_3 \cdot 2SiO_2)$, Titania (TiO_2) , and polystyrene, aimed to enhance thermal insulation. The XRD test was also conducted on Sample S5, which included the same compounds with magnesium oxide (MgO) to increase thermal insulation. The results confirmed the presence of the desired compounds in the samples, supporting their purpose of enhancing thermal insulation.

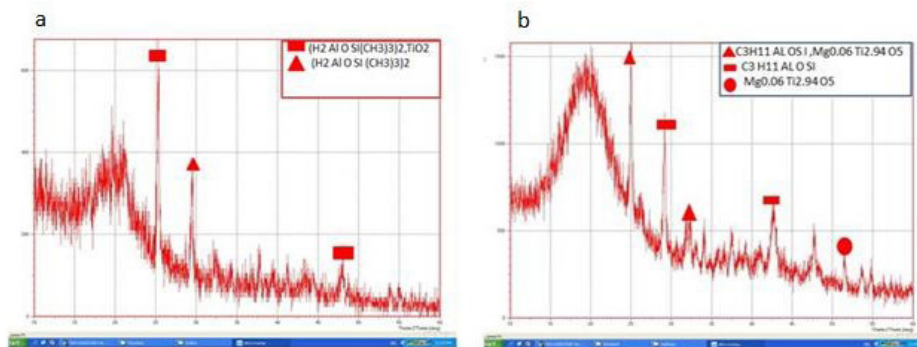


Figure 6. (a) The XRD analysis of the S4 sample to increase insulation by containing alumina, silicate (from the Mullite), titanium dioxide, and carbon, oxygen, and hydrogen (from polystyrene), (b) the X-R-D test analysis for S5 sample to increase the insulation contain alumina, silicate (from the Mullite), titanium dioxide, Magnesium oxide, and carbon, oxygen, hydrogen (from polystyrene)

Morphology Properties

Scanning Electron Microscopy (SEM) test: SEM images reveal the presence of mullite grains and TiO₂ grains in sample S4, as well as the cross-section of the coating. Likewise, the SEM images of sample S5 show the same compounds with magnesium oxide. SEM images show increased porosity, leading to decreased thermal conductivity.

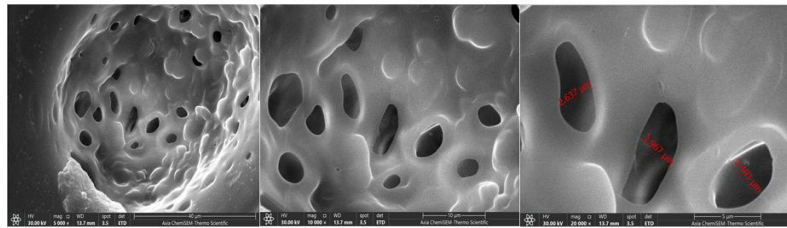


Figure 7. SEM test for S1 without adding ceramic materials

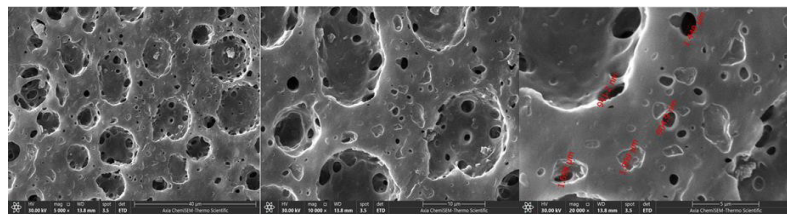


Figure 8. SEM test for S4 containing percentage of (Mullite and TiO₂)

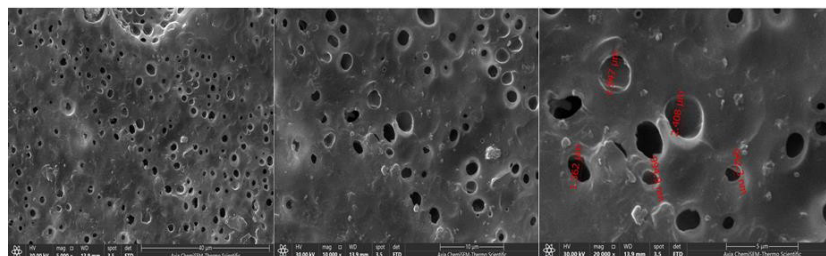


Figure 9. SEM test for S4 contains a percentage of (mullite, TiO₂ and MgO)

Atomic Force Microscopy (AFM) test: the AFM test was conducted on thermal insulation samples: S4, containing mullite and titanium oxide (TiO₂), and S5, containing mullite, titanium oxide (TiO₂), and magnesium oxide (MgO). AFM analysis provided information about the surface morphology and properties of the samples at the nanoscale. It revealed details such as surface roughness, grain size, and distribution, which are crucial for understanding the thermal insulation performance. The addition of magnesium oxide in sample S5 may have introduced changes to the surface characteristics. AFM testing helps to assess the impact of these compounds on the thermal insulation properties and aids in optimizing material formulations.

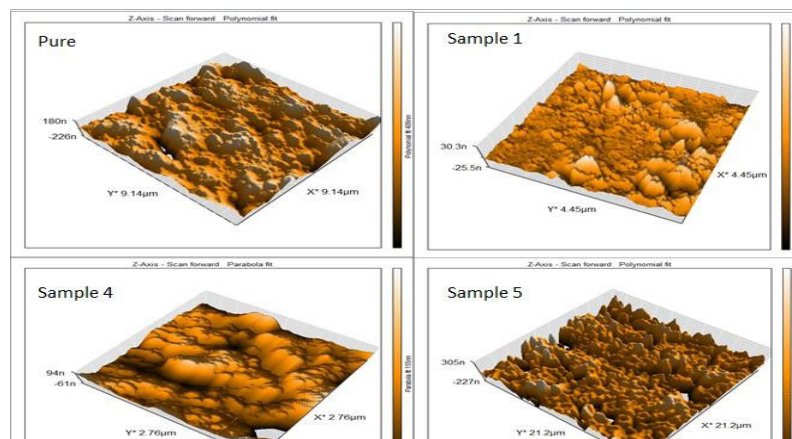


Figure 10. (AFM test) three dimension representation for the coating layer

Thermal Properties

Thermal conductivity test: is a valuable method for evaluating the dielectric properties of materials, including those containing mullite, titanium oxide (TiO₂) and magnesium oxide (MgO). By replacing a certain proportion of mullite with titanium oxide and magnesium oxide, the thermal conductivity of the samples can be modified to evaluate the effect on insulation. The results will indicate whether replacing mullite with titanium oxide at a rate of 1 % led to a noticeable decrease in thermal conductivity and improved insulation in sample S2. The same materials were also added at a rate of 3 % to obtain an increase in insulation. In addition, it is reported that insulation was increased by replacing mullite with a higher percentage (5 %) of titanium oxide in sample S4 and for the same material replacement of 5 % with magnesium oxide in sample S5. This indicates a stronger focus on enhancing insulation properties. Thermal conductivity testing can be performed on these samples to determine the effect of increasing the replacement ratio on thermal conductivity and insulation performance. Low thermal conductivity indicates improved insulation and also indicates reduced heat transfer through the material. These results will help optimize the composition of the samples to enhance thermal insulation properties, based on the level of replacement required and the resulting thermal conductivity values. ASTM C177 provides guidelines and procedures for determining the steady-state thermal conductivity of various materials, including insulating coatings. The test involves using a guarded-hot-plate apparatus to measure the heat flux and temperature difference across the sample. This data is then used to calculate the thermal conductivity of the material.⁽²⁵⁾

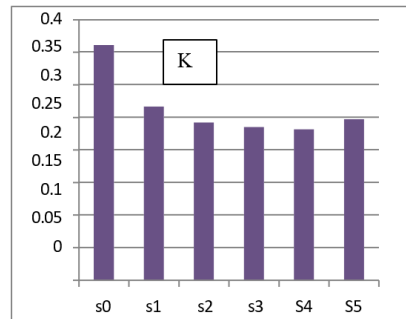


Figure 11. The decrease in thermal conductivity (k) for insulation samples

Table 2. Thermal conductivity test for samples to assess thermal insulation efficiency	
Samples No	Thermal conductivity K=w/m.c
S0 (pure)	0,360995
S1	0,266599
S2	0,242113
S3	0,234948
S4	0,231411
S5	0,2471976

Physical Properties

Density: density measurements were carried out on the samples to determine their respective densities. The lower density of sample S4 confirms its high porosity, which is associated with better thermal insulation.

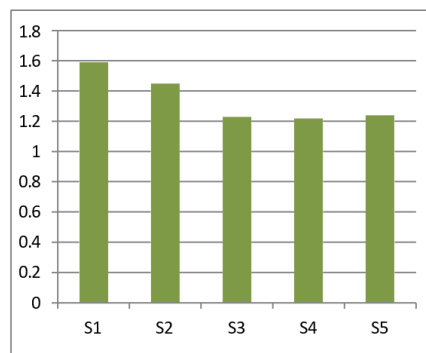


Figure 12. A measurement of density constant and the density of samples

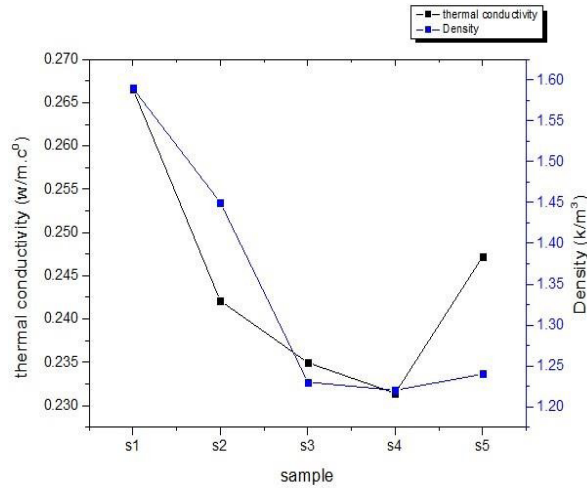


Figure 13. It shows the relationship between the thermal conductivity

Porosity: porosity measurements were conducted on the samples to assess their porosity levels Sample Sample S4 is characterized by a higher porosity than the rest of the samples, and this is consistent with what was mentioned above regarding density and thermal insulation, as it contains porous ceramic materials that increase thermal insulation.

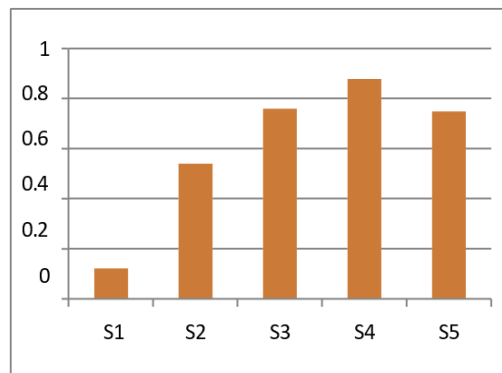


Figure 14. Porosity measurement constant and porosity of samples

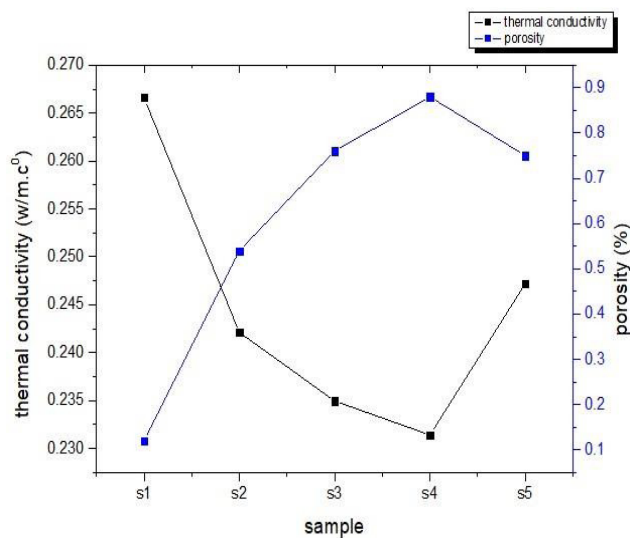


Figure 15. Explains the relationship between the thermal conductivity

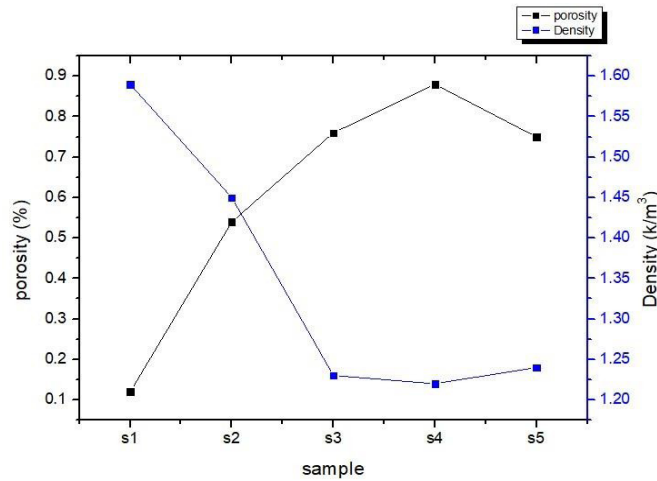


Figure 16. Explains the relationship between density and porosity of samples

The Archimedes method is used to measure density and porosity in paint. Approved standards such as ASTM D1475, ISO 2811-1, ISO 2811-2, and ASTM D4285 provide guidelines and procedures for conducting these measurements. These standards outline the equipment, sample preparation, measurement techniques, and calculations necessary for accurate density and porosity determination.⁽²⁶⁾

Coating thickness: the thickness of the insulating coating layer is important for insulation performance. It should be measured and controlled to get the best results. Note that sample S4 is the best coating thickness, and the increase in value of sample S5 is due to the addition of Magnesium oxide.

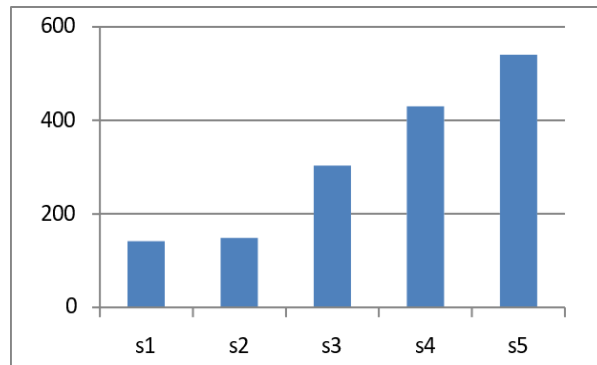


Figure 17. the coating thickness for insulation samples

Ultra-Violet (U.V) test: to increase thermal insulation, it is desirable to have low absorption, high reflection and high transmittance in the samples. This helps reduce heat transfer and improve energy efficiency. From the figure below it is clear that sample S4 is the best because it has low absorptivity, reflectivity and high transmittance, and this achieves good thermal insulation.

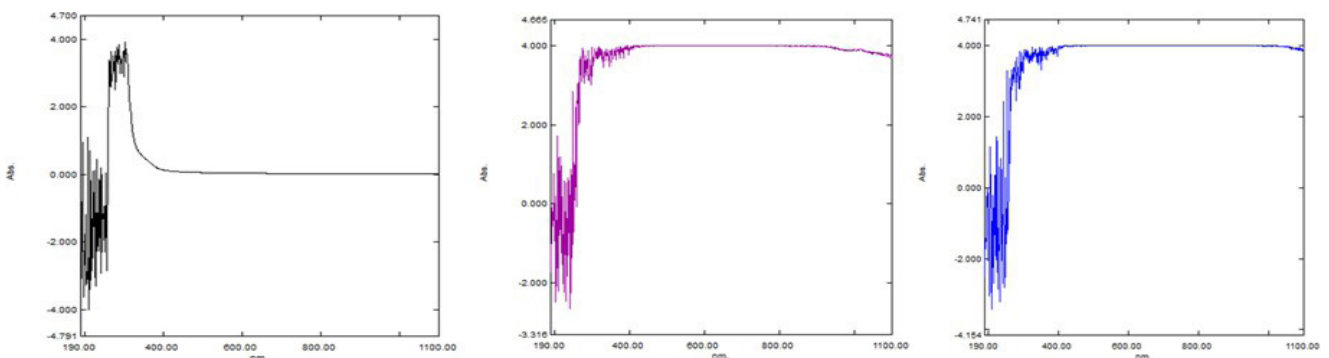


Figure 18. UV absorption test (a) for sample S1 without adding ceramic materials (b) for the sample with the highest percentage of S4 (mullite and TiO₂) (c) sample s5 containing a percentage of (mullite and TiO₂, MgO)

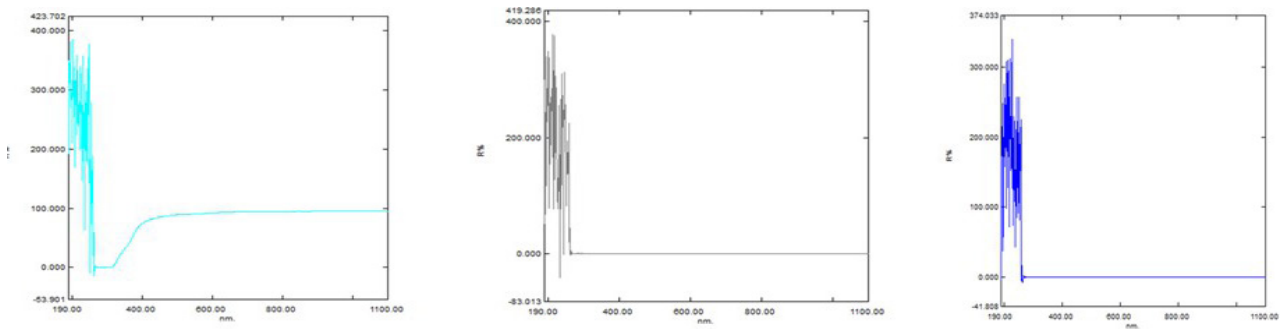


Figure 19. UV reflectance test (a) for sample S1 without adding ceramic materials (b) for sample with the highest percentage of S4 (Mullit and TiO₂) (c) sample S5 with a percentage of (mullite and TiO₂, MgO)

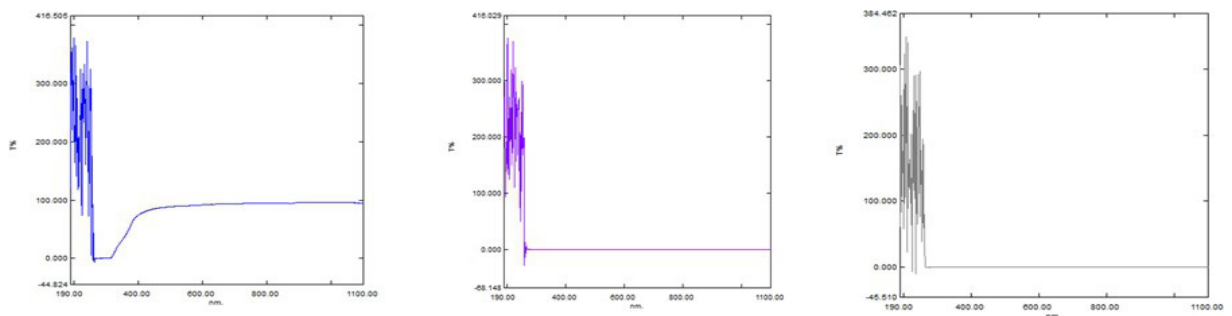


Figure 20. UV transmittance test (a) of sample S1 without addition of ceramic materials (b) of sample with highest percentage S4 (mullite and TiO₂) (c) sample S5 with percentage (mullite and TiO₂, MgO)

Mechanical properties

Adhesion strength test: adhesion strength is important for insulation samples to bond effectively with paint. Factors like surface preparation and material selection impact adhesion. Strong adhesion ensures paint remains intact, protecting insulation. The adhesion strength for insulation sample 4 is (15,29 MPa). The adhesion strength of paint samples can be tested using the PosiTest device, which measures the force required to detach a pull-off dolly from the painted surface. The device provides a quantitative measurement of adhesion strength and is widely used in quality control and inspection applications.

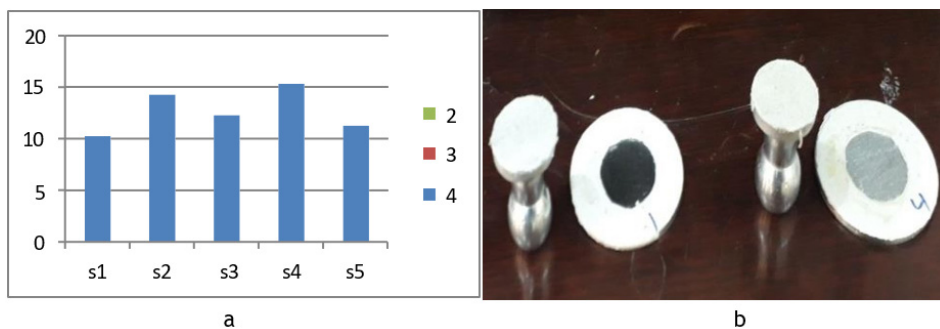


Figure 21. (a,b) the adhesion strength for insulation sample

CONCLUSIONS

- One of the promising methods for water desalination is to take advantage of renewable energy sources, especially sunlight.
- Ceramic materials, including mullite, titanium oxide, and magnesium oxide, have shown promising results in thermal insulation applications. These materials offer potential benefits in terms of reducing thermal conductivity and enhancing insulation capabilities. By incorporating these ceramics into insulation compositions, heat transfer can be reduced to a minimum, resulting in improved thermal resistance. The use of ceramic materials for insulation purposes has been supported by their unique properties and compositions, which has been confirmed through various tests and analyses. These results contribute to the continuous development and improvement of ceramic-based thermal insulation materials, which have the potential to significantly improve energy efficiency and thermal management in various applications.

Adding polyester resins to paint can increase adhesion and durability.

- The stainless steel base is painted with spray painting technology. By controlling the distance, air pressure, and coating speed, a uniform and homogeneous coating is achieved, which enhances corrosion resistance.

- Among the tests used are: XRD (X-ray diffraction): determines the chemical composition and crystalline structure of materials. SEM (Scanning Electron Microscope): Provides high-resolution images of the surface, revealing microstructure and morphology. AFM (Atomic Force Microscopy): Measures surface roughness, morphology and topography with high precision. Thermal conductivity: evaluates the changes in heat transfer caused by the coating. Density and Porosity: Determines the density of the coating and the level of porosity. Coating Thickness: measures the thickness of the applied coating. Ultraviolet (UV): evaluates the absorption, transmission and transmittance properties of the coating to protect against UV rays. Adhesion: Tests the strength and durability of the bond between the coating and the substrate.

- Sample S4 of the 316 stainless steel sink showed a higher insulation percentage compared to other samples. This conclusion was based on factors such as the presence of pores observed through SEM examination, low thermal conductivity, low density, and good adhesion to paint. These characteristics indicate that the coating on sample S4 provides effective insulation against heat transfer.

REFERENCES

1. M. A. F. Kurnianto, R. Irwansyah, L. Fabianto, A. Armadani, and Warjito, "Effect of Pressure on Salt Water Spray as Alternative Methods of Desalination Using Droplet Evaporation-Air Entrainment," *Int. J. Technol.*, vol. 14, no. 3, pp. 628-637, 2023, doi: 10.14716/ijtech.v14i3.5153.

2. J. Jiang et al., "We are IntechOpen, the world's leading publisher of Open Access books Built by scientists , for scientists TOP 1 %," *Intech*, vol. 34, no. 8, pp. 57-67, 2010, [Online]. Available: <https://doi.org/10.1007/s12559-021-09926-6><https://www.intechopen.com/books/advanced-biometric-technologies/liveness-detection-in-biometrics><http://dx.doi.org/10.1016/j.compmedimag.2010.07.003>

A. Sayigh, "Up-date: Renewable energy and climate change," *Renew. Energy Environ. Sustain.*, vol. 6, p. 13, 2021, doi: 10.1051/rees/2021004.

3. S. Gkalonaki and K. Karatzas, "Assessing the environmental impacts of renewable energy sources with emphasis on wind energy," *IOP Conf. Ser. Earth Environ. Sci.*, vol. 1123, no. 1, 2022, doi: 10.1088/1755-1315/1123/1/012053.

4. J. Yan et al., "Analysis of solar and wind power on access planning of multiple renewable energy sources," *IOP Conf. Ser. Earth Environ. Sci.*, vol. 621, no. 1, 2021, doi: 10.1088/1755-1315/621/1/012069.

5. Y. Si et al., "Preparation of lightweight corundum-mullite thermal insulation materials by microwave sintering," *Process. Appl. Ceram.*, vol. 15, no. 2, pp. 170-178, 2021, doi: 10.2298/PAC2102195Z.

6. B. Optical, "r Fo Pe er Re vi r Fo Pe Re vi," 2013.

7. K. P. Shejale, R. Krishnapriya, H. Patil, D. Laishram, P. Rawal, and R. K. Sharma, "Recent advances in ultra-low temperature (sub-zero to 100 °c) synthesis, mechanism and applications of titania (TiO₂) nanoparticles," *Mater. Adv.*, vol. 2, no. 23, pp. 7502-7529, 2021, doi: 10.1039/d1ma00942g.

8. R. R. Reeber, K. Goessel, and K. Wang, "Thermal expansion and molar volume of MgO, periclase, from 5 to 2900 K," *Eur. J. Mineral.*, vol. 7, no. 5, pp. 1039-1048, 1995, doi: 10.1127/ejm/7/5/1039.

9. Groza, "Advances in polymer based composite coatings," *Polymers (Basel).*, vol. 13, no. 10, pp. 4-6, 2021, doi: 10.3390/polym13101611.

10. P. Jelle, D. Arasteh, and C. Kohler, State-of-the-Art Highly Insulating Window Frames-Research and Market Review Project report 6-2007 SINTEF Building and Infrastructure Project report no 6 Arild Gustavsen 1) 2) State-of-the-Art Highly Insulating Window Frames-Research and Market Review spec. 2007. [Online]. Available: www.sintef.no/byggforsk

11. J. Z. Lu, W. W. Deng, K. Y. Luo, L. J. Wu, and H. F. Lu, "Surface EBSD analysis and strengthening mechanism of AISI304 stainless steel subjected to massive LSP treatment with different pulse energies," *Mater.*

Charact., vol. 125, pp. 99-107, 2017, doi: 10.1016/j.matchar.2017.01.036.

12. Latifi, M. Imani, M. T. Khorasani, and M. Daliri Joupari, "Plasma surface oxidation of 316L stainless steel for improving adhesion strength of silicone rubber coating to metal substrate," *Appl. Surf. Sci.*, vol. 320, pp. 471-481, 2014, doi: 10.1016/j.apsusc.2014.09.084.

13. S. Luangkularb, S. Prombanpong, and V. Tangwarodomnukun, "Material consumption and dry film thickness in spray coating process," *Procedia CIRP*, vol. 17, pp. 789-794, 2014, doi: 10.1016/j.procir.2014.02.046.

14. Y. H. Huang, L. C. Chen, and H. M. Chou, "Optimization of process parameters for anti-glare spray coating by pressure-feed type automatic air spray gun using response surface methodology," *Materials (Basel)*., vol. 12, no. 5, 2019, doi: 10.3390/ma12050751.

15. Y. Pan, "Research Progress and Application Status of Thermal Insulation Coatings," *IOP Conf. Ser. Earth Environ. Sci.*, vol. 295, no. 3, 2019, doi: 10.1088/1755-1315/295/3/032048.

16. D. B. Container, "(12) Patent Application Publication (10) Pub. No.: US 2015/0327727 A1," vol. 1, no. 19, 2015.

17. S. Samal, J. Kopeček, and P. Šittner, "Interfacial Adhesion of Thick NiTi Coating on Substrate Stainless Steel," *Materials (Basel)*., vol. 15, no. 23, 2022, doi: 10.3390/ma15238598.

18. S. O. Driscoll, "Magnesium Oxide Use as a Pigment in Coating Formulations," *Chem. Pap. Eng.*, pp. 4-21, 1996.

19. R. V. R. Verma, S. K. S. Kumar, N. M. S. N. M. Suri, and S. K. S. Kant, "Optimization of Mullite Based Coating Using Slurry Spray Technique," *Int. J. Sci. Res.*, vol. 2, no. 8, pp. 166-169, 2012, doi: 10.15373/22778179/aug2013/56.

20. D. Ge, M. Shi, Y. Yao, S. Jiang, and D. He, "Preparation and Properties of Anti-Insulation Integrated Phenolic Resin Composites Preparation and Properties of Anti-Insulation Integrated Phenolic Resin Composites", doi: 10.1088/1757-899X/472/1/012047.

21. K. Viswajeet, B. K. Yadav, and P. Kumar, "Single Basin Solar Still Using Different Absorbing Material Part: a Review," *Int. J. Eng. Appl. Sci. Technol.*, vol. 04, no. 10, pp. 167-169, 2020, doi: 10.33564/ijeast.2020.v04i10.032.

22. R. N. Taqi, Z. A. Abdul Redha, and F. I. Mustafa, "Experimental Investigation of a Single Basin - Single Slope Solar Still Coupled with Evacuated Tube Solar Collector," *J. Eng.*, vol. 27, no. 6, pp. 16-34, 2021, doi: 10.31026/j.eng.2021.06.02.

23. S. Shalaby, A. E. Kabeel, B. E. Moharram, A. Shama, and H. A. Abosheisha, "Experimental study on the single basin solar still integrated with shell and spiral finned tube latent heat storage system enhanced by copper oxide nanoparticles," *Environ. Sci. Pollut. Res.*, vol. 30, no. 10, pp. 27458- 27468, 2023, doi: 10.1007/s11356-022-24104-3.

24. R. Clarke, G. Rosengarten, and B. Shabani, "Flexible Buffer Materials to Reduce Contact Resistance in Thermal Insulation Measurements," *Proc. 32nd Int. Therm. Conduct. Conf. 20th Int. Therm. Expans. Symp.*, pp. 64-73, 2014, doi: 10.5703/1288284315544.

25. S. Bai, N. Perevoshchikova, Y. Sha, and X. Wu, "The effects of selective laser melting process parameters on relative density of the AlSi10Mg parts and suitable procedures of the archimedes method," *Appl. Sci.*, vol. 9, no. 3, 2019, doi: 10.3390/app9030583.

FINANCING

The authors did not receive financing for the development of this research.

CONFLICT OF INTEREST

The authors declare that there is no conflict of interest.

AUTHORSHIP CONTRIBUTION

Conceptualization: Elham A. Majeed, Hayder K. Rashid, Saja F. Abdul Hadi.

Data curation: Elham A. Majeed, Hayder K. Rashid, Saja F. Abdul Hadi.

Formal analysis: Elham A. Majeed, Hayder K. Rashid, Saja F. Abdul Hadi.

Research: Elham A. Majeed, Hayder K. Rashid, Saja F. Abdul Hadi.

Methodology: Elham A. Majeed, Hayder K. Rashid, Saja F. Abdul Hadi.

Drafting - original draft: Elham A. Majeed, Hayder K. Rashid, Saja F. Abdul Hadi.

Writing - proofreading and editing: Elham A. Majeed, Hayder K. Rashid, Saja F. Abdul Hadi.